Journal of Nuclear Materials 451 (2014) 82–87

Contents lists available at ScienceDirect

Journal of Nuclear Materials

journal homepage: www.elsevier.com/locate/jnucmat

Interaction of carbon–vacancy complex with minor alloying elements of ferritic steels

A. Bakaev [a,b,c,*], D. Terentyev [a], X. He [d], E.E. Zhurkin [c], D. Van Neck [b]

[a] SCK•CEN, Nuclear Materials Science Institute, Boeretang 200, Mol B2400, Belgium
[b] Center for Molecular Modeling, Department of Physics and Astronomy, Ghent University, Technologiepark 903, 9052 Zwijnaarde, Belgium
[c] Department of Experimental Nuclear Physics K-89, Institute of Physics, Nanotechnology and Telecommunications, St. Petersburg State Polytechnical University, 29 Polytekhnicheskaya Str., 195251 St. Petersburg, Russia
[d] China Institute of Atomic Energy, P.O. Box 275-51, 102413 Beijing, China

ARTICLE INFO

Article history:
Received 24 January 2014
Accepted 19 March 2014
Available online 26 March 2014

ABSTRACT

Interstitial carbon, dissolved in bcc matrix of ferritic steels, plays an important role in the evolution of radiation-induced microstructure since it exhibits strong interaction with vacancies. Frequent formation and break-up of carbon–vacancy pairs, occurring in the course of irradiation, affect both kinetics of the accumulation of point defect clusters and carbon spatial distribution. The interaction of typical alloying elements (Mn, Ni, Cu, Si, Cr and P) in ferritic steels *used* as structural materials in *nuclear* reactors with a carbon–vacancy complex is analyzed using *ab initio* techniques. It is found that all the considered solutes form stable triple clusters resulting in the increase of the total binding energy by 0.2–0.3 eV. As a result of the formation of energetically favourable solute–carbon–vacancy triplets, the dissociation energy for vacancy/carbon emission is also increased by ~0.2–0.3 eV, suggesting that the solutes enhance thermal stability of carbon–vacancy complex. Association of carbon–vacancy pairs with multiple solute clusters is found to be favorable for Ni, Cu and P. The energetic stability of solute(s)–carbon–vacancy complexes was rationalized on the basis of pairwise interaction data and by analyzing the variation of local magnetic moments on atoms constituting the clusters.

1. Introduction

Fe-based steels with body centered cubic (BCC) structure such as bainitic or high-Cr ferritic–martensitic ones are the common structural materials for nuclear applications [1]. During operation the steels undergo degradation due to the harsh exploitation conditions. Radiation-induced embrittlement is one of the limiting factors determining safety and effective exploitation of a nuclear setup (see e.g. [1,2]). The embrittlement is conventionally attributed to the obstruction of dislocation movement by nanometric lattice defects formed as a result of radiation-induced/enhanced segregation and accumulation of point defect clusters growing to the dislocation loops and nano-voids [2].

Recent experimental studies involving several high resolution techniques including atom probe tomography (APT) emphasize the presence of solute-rich clusters (SRC), composed of major alloying elements, revealed in different types of commercial steels [3–8]. Remarkably, all the mentioned experimental works report extremely high density of SRC (up to 10^{24} m^{-3}). Due to their small size, these clusters are invisible to transmission electron microscopy (TEM).

The APT techniques, however, cannot determine the full structure of the SRCs and therefore their possible association with radiation-induced lattice defects remains unknown. Specially dedicated atomistic study addressing segregation in Fe–Mn–Ni–Cu alloys – a model for reactor pressure vessels (RPV) steel, has suggested that non-equilibrium formation of SRCs can be explained by their association with in-cascade created dislocation loops [9]. In line with that, the association of Mn and Si (important solutes entering RPV steels) with self-interstitial atoms resulting in highly stable configurations was also recently proven by *ab initio* calculations [10]. However, a combination of APT and positron annihilation spectroscopy (PAS) analysis also revealed the presence of vacancy-rich SRC complexes [11,12] in both western and Russian types of RPV steels. Hence, the mechanism of nucleation of SRCs on vacancies also needs to be clarified.

Investigation of vacancy-type defects in Fe-based steels cannot be carried without consideration of carbon, which has a great impact on the stability and mobility of vacancies in BCC Fe matrix [13,14]. Carbon atoms are dissolved in BCC iron matrix as

* Corresponding author at: SCK•CEN, Nuclear Materials Science Institute, Boeretang 200, Mol B2400, Belgium. Tel.: +32 486685042.
E-mail address: abakaev@sckcen.be (A. Bakaev).

http://dx.doi.org/10.1016/j.jnucmat.2014.03.031
0022-3115/

interstitial impurities and occupy octahedral sites in the equilibrium lattice [15]. Rigorous *ab initio* calculations have confirmed experimental observations that interstitial carbon (C) is strongly bound to a single vacancy [15] and multiple highly stable carbon–vacancy (C–V) complexes can grow further [16]. Although different *ab initio* codes and methods exhibit some discrepancies in terms of the absolute values of the C–V interaction energies (see analysis in [17,18]), qualitatively they all convey to the same message: mobility and stability of vacancies and small vacancy clusters are defined by the amount of interstitial carbon dissolved in a matrix.

Earlier *ab initio* works dedicated to study of solute alloying elements in bcc Fe also reveal the positive binding energy (i.e. attractive interaction) for several elements with vacancies [19–21], which is especially strong for Cu, Si and P. An interstitial carbon, however, repels most of the studied solutes (Mo, W, Nb, Ta, V, Si, Cr) except for Mn. But in the case of Cu–vacancy–carbon cluster it has been demonstrated that a single vacancy may act as bounding chain for carbon–solute complex, so that the simultaneous presence of Cu–C pair enhances thermal stability of Cu–C–vacancy complex [22]. This result might provide a hint for the nucleation of thermally stable solute–carbon–vacancy (S–C–V) clusters observed in the afore mentioned APT studies.

In this work we therefore perform a parametric *ab initio* study to investigate thermal stability of S–C–V complexes and consider a main set of alloying elements entering the composition of RPV steels, namely: Mn, Ni, Cu, Si, Cr and P. The density functional theory (DFT) method offers an efficient way to consider the energetic stability of small SRC clusters and to validate possible synergetic effects of vacancy–carbon and vacancy–solute binding. Correspondingly, we apply this tool and use exactly the same parameterization (except for the higher cut-off plane wave energy which is necessary for a system with a carbon atom) as in the earlier studies [19,21] to have fully compatible results with the already published data. The main purpose of the work is therefore to identify S–C–V structures with the lowest energy, compute the corresponding binding and dissociation energy of such complexes, and examine evolution of the incremental binding energy by addition of extra solutes to stable S–C–V clusters.

2. Computational details

The DFT calculations were performed with the Vienna Ab Initio Simulation Package VASP [23,24] using the projector-augmented wave (PAW) potentials [25,26]. The electron exchange–correlation functional was described within the generalized gradient approximation using PW91 functionals [27], with a Vosko–Wilk–Nusair interpolation [28]. For Fe, Cr, Mn, Si, Ni, Cu, P and C pseudo potentials with 8, 6, 7, 4, 10, 11, 5 and 4 valence electrons were used, respectively. Ionic relaxation was performed using the conjugate gradient algorithm with a force convergence criterion of 0.03 eV/Å. All the calculations were done keeping the cell shape and volume (equal to the equilibrium volume of bulk iron) constant. The energy cutoff for calculations was 450 eV which was checked to be enough to provide converged results. A $3 \times 3 \times 3$ k-point mesh was sampled by the Monkhorst and Pack scheme for systems with 128 atoms. The lattice parameter of pure ferromagnetic Fe is taken to be 2.831 Å following the previous studies [19,21].

Given that we perform spin-polarized calculations in the ferromagnetic system and introduce an anti-ferromagnetic impurity (i.e. Mn), one needs to be careful when selecting the initial value of the magnetic moment to ensure that the true minimum energy configuration is obtained after the relaxation. For the configurations involving Mn, we performed additional calculations varying the absolute value and sign of the initial magnetic moment of Mn as some of the results turned out to be particularly sensitive to this choice. Below, we report the results corresponding to the lowest energy configurations only.

To assess the binding energy we apply standard definition conventionally used in many similar DFT works [19]. The binding energy of n defects $\{A_i\}$ is defined as [19]:

$$E_b(\{A_i\}) = \sum_{i=1}^{n} E(A_i) - [E(\{A_i\}) + (n-1)E_0], \quad (1)$$

where $E(A_i)$ is the energy of the configuration containing A_i only, $E(\{A_i\})$ is the energy of the configuration with all the n defects and E_0 refers to a configuration containing no defects or impurities, i.e. bulk bcc iron. Following this notation, a positive value implies an attractive interaction and vice versa.

Considering defect clusters the term 'total interaction energy' refers to the energy which is necessary to separate all the defects away from a cluster. In practice, the dissolution of a complex cluster takes place by consecutive emission of its constitutes and characterization of the energy barrier for that process requires introduction of another term. The energy to remove one entity forming a cluster consisting of N objects will be called *the incremental binding energy* of an object #1 to $N-1$ cluster and will be referred to as E_b^1. If the removal of a single entity (e.g. object #1) from a cluster (containing e.g. three objects) results in the formation of a repulsive configuration (e.g. object #2 repels object #3), the incremental binding energy for object #1 is considered to be equal to the total binding energy of the cluster 1–3.

3. Results and discussion

Characterization of a possible synergetic effect of solute–carbon–vacancy interaction requires subdivision of the interaction energy between different entities and its estimation as a function of mutual spacing. This section therefore contains five subsections dedicated to the study of carbon–vacancy, solute–solute, solute–vacancy, solute–carbon and solute–carbon–vacancy in one cluster. For the sake of briefness, we shall use the notations S, C and V for the considered constitutes.

3.1. Carbon–vacancy interaction

Using the above described DFT parameterization set, we have recalculated the vacancy–carbon interaction energy which was found to be 0.70 eV, being the maximum value at the distance of $a_0/2$ between C and vacancy. This value is close to 0.64 eV, which was deduced using the formation energies reported by Forst et al. in [16]. In that work, a larger supercell was used, which eventually explains the deviation of 0.06 eV [16]. Note that the earlier study of Domain et al. reports rather low value of the C–V binding energy, namely 0.47 eV [15]. The reason for the discrepancy with our calculations and results of Forst et al. is discussed in [17].

In the discussion below, we will refer to the migration energy for carbon which is taken to be 0.92 eV as estimated by Domain et al. [15], being very close to the experimental values of 0.88 eV [29] and 0.85 eV [30]. We will use the value for the vacancy migration energy of 0.65 eV [31], which was obtained by VASP with a similar parameterization as here. Thus, the dissociation of the vacancy–carbon pair is to occur via emission of a vacancy (for details see [17]) and the corresponding dissociation energy is $E_d = 1.35$ eV, conventionally calculated as a sum of the binding energy and the migration energy (of the emitting specie).

3.2. Solute–solute interaction

The S–S interaction at the distance of 1nn (first nearest neighbour) and 2nn (second nearest neighbour) is shown in Fig. 1. As calculated in [19,21] there is an attractive binding energy between a pair of Mn or Cu atoms at the 1nn position which vanishes at the 2nn distance. The pairs of P atoms, for which we performed additional calculations, repel each other at 1nn distance and the repulsion is negligible at the 2nn distance. Si–Si or Cr–Cr form strongly repelling configurations in the both 1nn and 2nn positions. Ni shows negligible interaction with another Ni atom added in either 1nn or 2nn position.

3.3. Solute–vacancy interaction

The S–V binding energy as a function of distance is presented in Fig. 2. All the considered solutes exhibit attractive interaction with the vacancy which vanishes at the 3nn distance. Ni is, however, the only element showing non-monotonic binding energy, with the maximum in the 2nn position. P and Si reveal the strongest interaction energy to a vacancy (0.38 eV and 0.29 eV, respectively), which are 3p elements and therefore have strong contribution to the magnetic disorder. While, Cr and Ni show the weakest interaction (binding up to 0.1 eV), although Ni binds stronger in the 2nn position. Mn and Cu exhibit moderate binding energy in the range 0.16–0.26 eV.

3.4. Solute–carbon interaction

The solute–carbon interaction, presented in Fig. 3a, was inspected by placing a carbon atom in each octahedral position within the 5th nearest neighbour distance from the solute. The interaction vanishes to zero at the distance of $3/2a_0$ and is strongly repulsive for all the solutes except for Mn. Previously, the attractive interaction for Mn–carbon was also reported in [32]. It is also important to mention that Si and P exhibit outstandingly strong repulsive interaction with carbon being initially placed at a distance of $0.75–0.90a_0$. The interaction energy for all the other elements monotonically descents with the S–C distance.

In the calculations involving Mn atom, we have attempted several initial guesses for the Mn spin (both co- and anti-aligned with Fe atoms). The lowest energy configuration, revealing weak but attractive interaction, was obtained for the ferromagnetic spin orientation. The displacement of carbon atom from its perfect octahedral position after the complete relaxation of Mn–C pair (see Fig. 3b) was practically negligible, while we observed a significant shift of the magnetic moment on Mn atom (by +2.75 μ_B, see Fig. 3(d)). The observed effect might therefore be related to the peculiar magnetic relaxation of anti-ferromagnetic manganese inside the ferromagnetic iron matrix in the vicinity of carbon, which introduces certain magnetic disturbance/disorder on magnetic behaviour of Fe atoms.

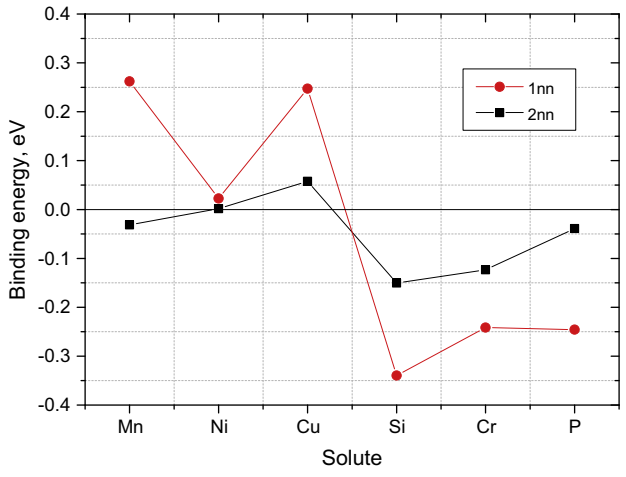

Fig. 1. Solute–solute binding energy.

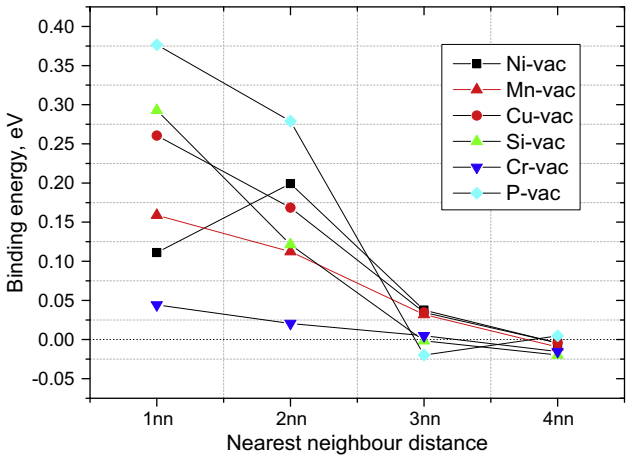

Fig. 2. Solute–vacancy binding energy.

The relaxation-induced displacement of the carbon and other solute atoms as well as the change of their magnetic moments are shown in Fig. 3(b)–(e). One can see that the solute displacement for the interaction with carbon in the 1nn is practically similar for all the solutes, except for P atom, and the displacement essentially drops in the 2^{nn} position (and for larger distances). The displacement of carbon atom, on the other hand, depends greatly on the solute type and in the case of P, Si, Cr, Mn and Cu it is higher for the 2nn position than for the 1nn one. Consistently, Si–C and P–C interaction is found to be stronger in the 2nn pair. The strong repulsion for Si–C and P–C pairs should therefore be attributed to the elastic interaction.

3.5. Solute–vacancy–carbon complexes

Following the above presented data for the pair interaction of different constitutes, one can anticipate the structure of the most favourable S–C–V clusters. As the carbon–vacancy interaction is expected to provide the highest binding, the nuclei should involve this pair as shown in Fig. 4. Then, all the possible neighbourhood positions for a solute were considered accounting for the crystal symmetry. The complex with the lowest formation energy is shown in Fig. 4 and this configuration provides the lowest energy state for all the studied solutes. The cluster structure represents itself a triangle, where the vacancy stands as 1nn to a solute, while the S–C distance is $\sqrt{6}/2a_0 \approx 1.2a_0$.

The total and incremental binding energies for S–C–V clusters as well as the dissociation energies are shown in Fig. 5. The two straight solid lines reveal the V–C binding and dissociation energy to provide the reference and underline the synergetic effect of the solute addition. Following the energy balance, one reveals that the emission of a vacancy from all the complexes (except for Mn–V–C) results in the formation of the repulsive carbon–solute pair. For those cases the incremental binding energy $E_b^I(CS + V)$ is considered to be equal to the total binding energy $E_b(S + V + C)$. In the case of Mn solute the incremental binding energy $E_b^I(CMn + V)$ is equal to 0.80 eV. From Fig. 5 it clearly follows that the total binding energy $E_b(S + V + C)$ is essentially higher than solute–vacancy binding energy $E_b(S + V)$ and lays above the vacancy–carbon binding

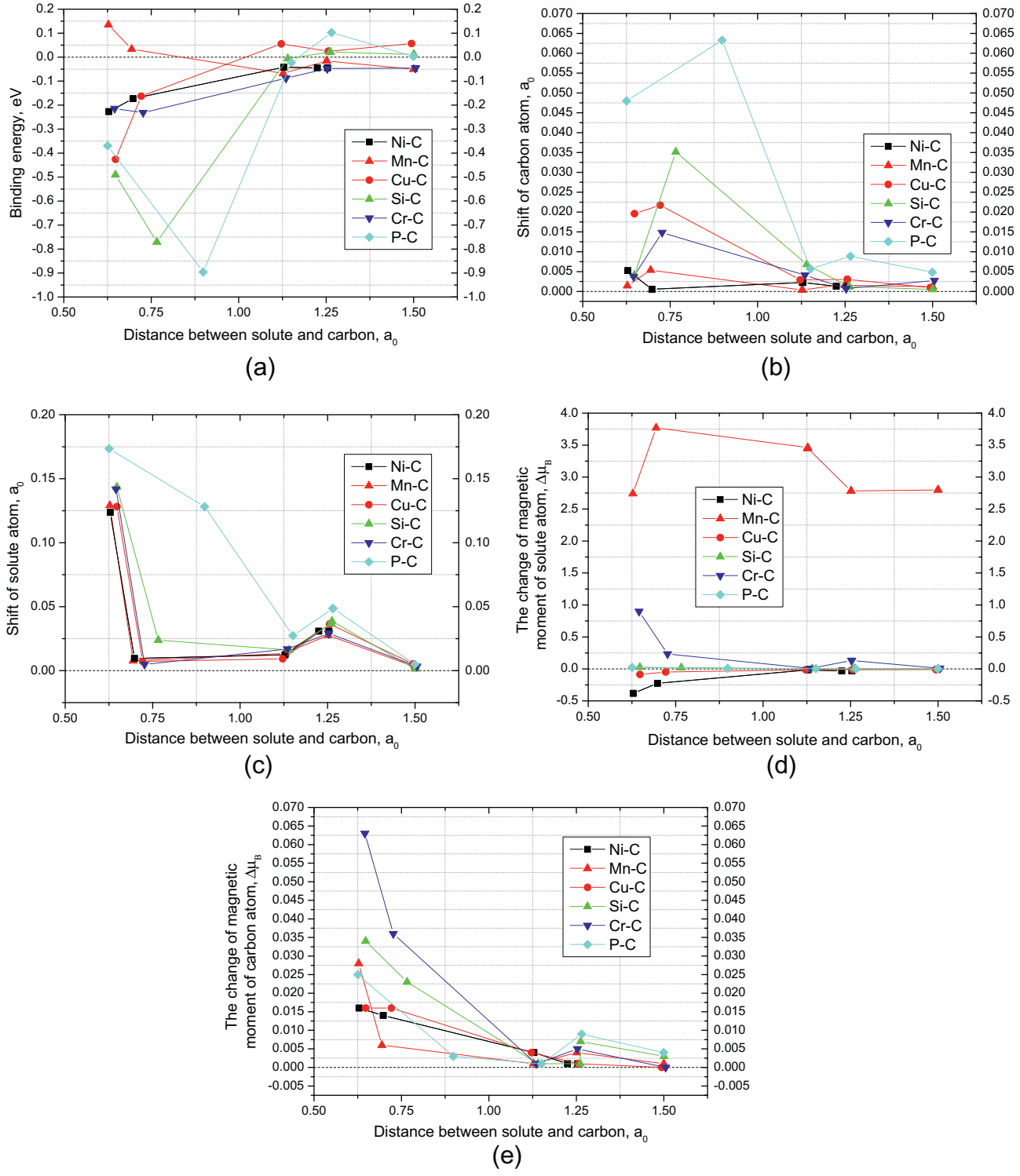

Fig. 3. (a) Solute–carbon binding energy. Displacement of (b) carbon atom and (c) solute atom obtained after the relaxation of solute–carbon pair. Change of magnetic moments of (d) solute and (e) carbon atoms obtained after the relaxation of solute–carbon pair.

energy E_b(V + C) value. The incremental binding energy of carbon in the triple complex E_b^{I}(VS + C) is approximately the same as its binding with vacancy E_b(V + C).

Due to the increase of the binding of a vacancy in the triple complex (as compared to V–C) by approximately 0.2–0.3 eV the dissociating specie in the triple complex (either carbon or vacancy) will be defined by the type of the solute constituting the cluster. The dissociation energies for a vacancy and carbon from each of the considered S–V–C complexes are compared in Fig. 5.

The dissociation by the emission of an interstitial carbon requires a lower energy barrier than for a vacancy in the case of phosphorus–V–C complex. While for Ni-, Cr- and Mn-containing clusters the dissociation is more likely to occur by the emission of a vacancy, leading to subsequent breakup of the S–C pair. The dissociation by either of the species is equally probable in the case

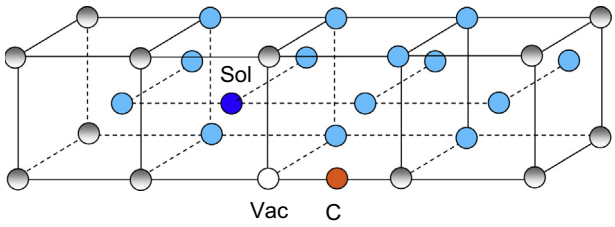

Fig. 4. Considered configurations of solute–vacancy–carbon complexes. Light blue atoms refer to the studied positions of a solute. The dark-blue-coloured atom refers to the lowest energy configuration. Non-filled circle refers to the position of a vacancy. The carbon atom is shown by an orange circle. (For interpretation of the references to colour in this figure legend, the reader is referred to the web version of this article.)

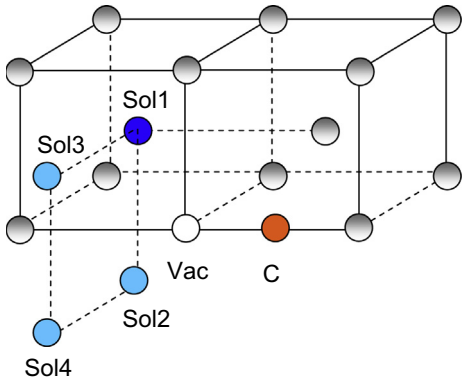

Fig. 6. The schematic picture of larger solute–vacancy–clusters considered.

of Cu and Si. Overall, we see that the dissociation barrier for the S–C–V clusters is by about 0.3 eV higher than E_d(V–C). Hence, the association of vacancies and carbon with any of the studied solutes leads to a higher thermal stability of V–C pairs.

3.6. Addition of extra solutes (up to three) to vacancy–solute–carbon complex

To explore a mechanism of growth of an elementary S–C–V complex and possibility for a multiple trapping, we have considered the addition of extra solutes (up to three) in the equivalent positions and have verified if the inclusion results in a deeper trapping of the mobile species (i.e. C and V). The structures of the inspected clusters are presented in Fig. 6, where all three additional positions are equivalent to the position 'Sol1' with respect to the orientation of the C–V complex.

Firstly, we consider the interaction energy for the extra solutes added to the S–C–V complex. Fig. 7 presents the binding energy of the nth solute to S_{n-1}–C–V complex. So far, we have considered S_n–C–V complexes containing solutes of the same kind. Clearly, all the considered clusters will gain energy by absorbing at least one more solute. However, Mn-, Si- and Cr- containing clusters are not expected to accept the third solute. This can be explained by the solute–solute repulsive interaction taking place for the Cr–Cr and Si–Si pairs. The explanation for the repulsion of 3rd and 4th Mn atom from Mn_2–V–C cluster requires further investigation. It is very likely that the energetic stability of larger Mn-, Cr- and Si- rich clusters could be realized by further addition of vacancies and carbon atoms.

Ni-, Cu- and P-made clusters on the contrary keep gaining the energy as more solutes are added. In the case of Cu, the attractive interaction is consistent with its extremely low solubility limit (in the calculations involving 1–4 Cu atoms its concentration is about 0.8 at.%, 1.6 at.%, 2.3 at.% and 3.1 at.%, respectively, while the solubility limit is below 0.2 at.% at the temperatures below 800 K [33,34]). P atom exhibits very strong positive binding energy to a vacancy, which eventually overwhelms a weaker P–P repulsive interaction, resulting in the energetically stable $P_{2,3,4}$–C–V complexes.

4. Summary and conclusions

In this work we have considered the stability of different solute–carbon–vacancy complexes exploring the solute atoms (Mn, Ni, Cu, Si, Cr and P) entering a composition of typical commercial ferritic steels used as structural nuclear components (such as reactor pressure vessels or high-Cr ferritic/martensitic steels). The purpose of these calculations was to explore whether the formation of

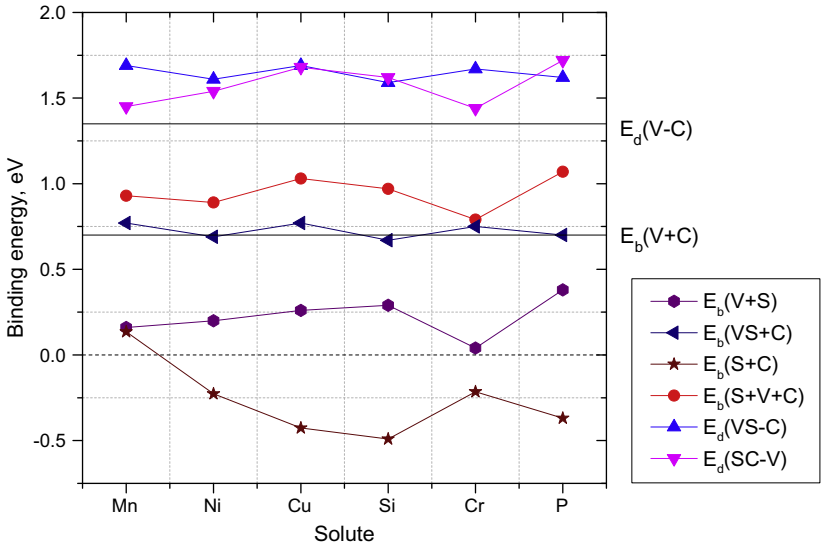

Fig. 5. Comparison of binding and dissociation energies. The following notations are used for: E_b(V + S) solute–vacancy binding energy, E_b(S + C) solute–carbon binding energy; E_b^I(VS + C) incremental binding energy of carbon to vacancy–solute pair; E_b(S + C + V) total binding energy of vacancy–solute–carbon complex; E_d(VS–C) and E_d(SC–V) dissociation energy of vacancy–solute–carbon cluster via the emission of carbon or vacancy, respectively. Black solid lines reveal the vacancy–carbon binding and dissociation energy in the absence of the interaction with solutes.

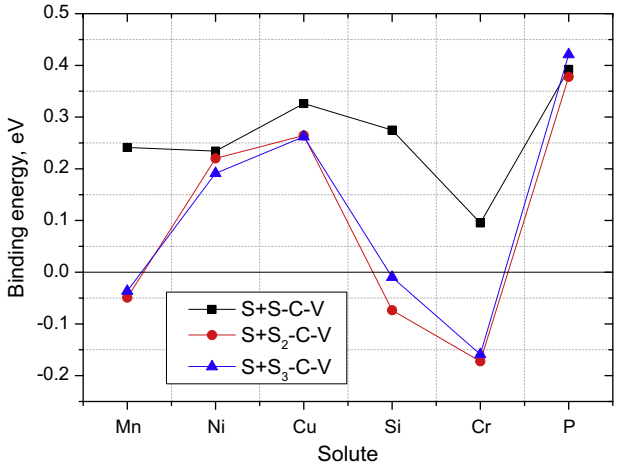

Fig. 7. The incremental binding energy of the nth solute to $S_{(n-1)}$–C–V cluster.

solute–carbon–vacancy complexes is energetically favourable process and to identify the optimal structures corresponding to the lowest energy using the DFT method. We found that all the considered solutes form stable S–C–V clusters, which have the same unique structure irrespective of the solute type. Based on the DFT results, the corresponding binding and dissociation energy for S–C–V triplets and the larger S_n–C–V (n = 2–4) complexes are calculated to examine the effect of the solutes on thermal stability of vacancies and carbon atoms.

The growth of the S–C–V complexes to S_2–C–V (with the same kind of solute) was found to be favourable for all the studied solutes, and Ni-, Cu- and P-containing clusters can accommodate up to three additional solutes. The growth of the Mn-, Cr- and Si-rich clusters is eliminated due to S–S or S–C repulsive interaction. However, the formation of thermally stable S_n–V–C containing mixed types of solutes cannot be ruled out and needs to be further explored.

The binding energy of an interstitial carbon to different S–V complexes is approximately the same as the V–C binding energy. However, the total binding energy is raised by about 0.2–0.3 eV for all the elements except for Cr. The presence of Mn, Cu and Cr slightly increases (by 0.1 eV) the binding energy of carbon to V–S complex, as compared to its binding to a vacancy in the C–V complex.

The dissociation of S–C–V clusters by the emission of an interstitial carbon requires a lower energy barrier than the one of a vacancy only in the case of P. While for Ni-, Cr-, Mn-containing clusters the dissociation is expected to happen by the detachment of a vacancy (leading to immediate breakup of the S–C pair in the case of Ni and Cr). The dissociation by either of the specie is equally probable in the case of Cu and Si. Overall, we see that the dissociation barrier for the S–C–V clusters is by about 0.2–0.3 eV higher than E_d(V–C), therefore the association of vacancies with any of the studied solutes leads to a stronger pinning of both freely migrating interstitial carbon and vacancies.

Acknowledgements

This work, supported by the European Commission under the Contract of Association between EURATOM/SCK-CEN, was carried out within the framework of the European Fusion Development Agreement. The computational resources (Stevin Supercomputer Infrastructure) and services used in this work were provided by the VSC (Flemish Supercomputer Center), funded by Ghent University, the Hercules Foundation and the Flemish Government – department EWI. Part of calculations has been performed at HPC Julich within the 'SORT' project. The research was partly supported by the FWO grant.

References

[1] R.L. Klueh, A.T. Nelson, J. Nucl. Mater. 371 (2007) 37–52.
[2] G.R. Odette, G.E. Lucas, Jom – J. Miner. Met. Mater. Soc. 53 (2001) 18–22.
[3] M.K. Miller, K.F. Russell, J. Nucl. Mater. 371 (2007) 145–160.
[4] Z. Jiao, G.S. Was, Acta Mater. 59 (2011) 1220–1238.
[5] G.S. Was, J.P. Wharry, B. Frisbie, B.D. Wirth, J. Nucl. Mater. 411 (2011) 41–50.
[6] E. Meslin, M. Lambrecht, M. Hernández-Mayoral, F. Bergner, L. Malerba, P. Pareige, B. Radiguet, A. Barbu, D. Gómez-Briceño, A. Ulbricht, A. Almazouzi, J. Nucl. Mater. 406 (2010) 73–83.
[7] V. Kuksenko, C. Pareige, P. Pareige, J. Nucl. Mater. 432 (2013) 160–165.
[8] Z. Jiao, G.S. Was, Acta Mater. 59 (2011) 4467–4481.
[9] G. Bonny, D. Terentyev, A. Bakaev, E.E. Zhurkin, M. Hou, D. Van Neck, L. Malerba, J. Nucl. Mater. 442 (2013) 282–291.
[10] A. Bakaev, D. Terentyev, X. He, D. Van Neck, J. Nucl. Mater. http://dx.doi.org/10.1016/j.jnucmat.2014.02.033.
[11] A. Kuramoto, T. Toyama, T. Takeuchi, Y. Nagai, M. Hasegawa, T. Yoshiie, Y. Nishiyama, J. Nucl. Mater. 425 (2012) 65–70.
[12] A. Kuramoto, T. Toyama, Y. Nagai, K. Inoue, Y. Nozawa, M. Hasegawa, M. Valo, Acta Mater. 61 (2013) 5236–5246.
[13] P. Hautojärvi, J. Johansson, A. Vehanen, J. Yli-Kauppila, Phys. Rev. Lett. 44 (1980) 1326–1329.
[14] P. Hautojarvi, L. Pollanen, A. Vehanen, J. Ylikauppila, J. Nucl. Mater. 114 (1983) 250–259.
[15] C. Domain, C. Becquart, J. Foct, Phys. Rev. B 69 (2004) 144112.
[16] C.J. Forst, J. Slycke, K.J. Van Vliet, S. Yip, Phys. Rev. Lett. 96 (2006) 175501.
[17] D. Terentyev, G. Bonny, A. Bakaev, D.V. Neck, J. Phys.: Condens. Matter. 24 (2012) 385401.
[18] 1998 Microstructural stability of creep resistant alloys for high temperature plant applications, IOM Communications, London.
[19] P. Olsson, T.P.C. Klaver, C. Domain, Phys. Rev. B 81 (2010) 054102.
[20] O.I. Gorbatov, P.A. Korzhavyi, A.V. Ruban, B. Johansson, Y.N. Gornostyrev, J. Nucl. Mater. 419 (2011) 248–255.
[21] A. Bakaev, D. Terentyev, G. Bonny, T.P.C. Klaver, P. Olsson, D. Van Neck, J. Nucl. Mater. 444 (2014) 237–246.
[22] B. Minov, M. Lambrecht, D. Terentyev, C. Domain, M.J. Konstantinovic, Phys. Rev. B 85 (2012).
[23] G. Kresse, J. Hafner, Phys. Rev. B 47 (1993) 558–561.
[24] G. Kresse, J. Furthmuller, Phys. Rev. B 54 (1996) 11169–11186.
[25] P.E. Blochl, Phys. Rev. B 50 (1994) 17953–17979.
[26] G. Kresse, D. Joubert, Phys. Rev. B 59 (1999) 1758–1775.
[27] J.P. Perdew, J.A. Chevary, S.H. Vosko, K.A. Jackson, M.R. Pederson, D.J. Singh, C. Fiolhais, Phys. Rev. B 46 (1992) 6671–6687.
[28] S.H. Vosko, L. Wilk, M. Nusair, Can. J. Phys. 58 (1980) 1200–1211.
[29] S. Takaki, J. Fuss, H. Kuglers, U. Dedek, H. Schultz, Radiat. Effects 79 (1983) 87–122.
[30] A. Vehanen, P. Hautojärvi, J. Johansson, J. Yli-Kauppila, P. Moser, Phys. Rev. B 25 (1982) 762–780.
[31] C. Domain, C. Becquart, Phys. Rev. B 65 (2002) 024103.
[32] N.I. Medvedeva, D.C.V. Aken, J.E. Medvedeva, J. Phys.: Condens. Matter. 23 (2011) 326003.
[33] G. Salje, M. Feller-Kniepmeier, J. Appl. Phys. 48 (1977) 1833–1839.
[34] M. Perez, F. Perrard, V. Massardier, X. Kleber, A. Deschamps, H. de Monestrol, P. Pareige, G. Covarel, Philos. Magn. 85 (2005) 2197–2210.